Contemporary Mathematics
https://ojs.wiserpub.com/index.php/CM/

Research Article

A Novel Romanovski-Jacobi Spectral Collocation Scheme for Fourth-Order ψ Fractional Sub-Diffusion Models

M. A. Abdelkawy[1*], A. Emin[2], Anjan Biswas[3,4,5]

[1] Department of Mathematics and Statistics, College of Science, Imam Mohammad Ibn Saud Islamic University (IMSIU), Riyadh, Saudi Arabia
[2] Department of Software Engineering, Istanbul Gelisim University, Istanbul 34310, Turkey
[3] Department of Mathematics and Physics, Grambling State University, Grambling, LA 71245-2715, USA
[4] Department of Physics and Electronics, Khazar University, Baku, AZ 1096, Azerbaijan
[5] Department of Mathematics and Applied Mathematics,Sefako Makgatho Health Sciences University Medunsa, Pretoria 0204, South Africa
E-mail: maohamed@imamu.edu.sa

Received: 30 June 2025; **Revised:** 19 November 2025; **Accepted:** 4 December 2025

Abstract: This paper presents a novel Romanovski-Jacobi (R-J) spectral collocation scheme for numerically solving Fourth-Order ψ-Fractional Sub-Diffusion models (FO-ψFSDEs). These models, which are governed by ψ-fractional differential equations, play a crucial role in accurately capturing memory and hereditary properties in complex anomalous diffusion phenomena, particularly in physics and biology. Due to the analytical complexity of such equations, the development of efficient numerical methods is essential. The proposed R-J Spectral Collocation (RJSC) approach leverages the orthogonality and localization properties of R-J polynomials to construct highly accurate approximations. The study demonstrates the robustness and precision of the method through several benchmark examples, emphasizing its potential for modeling and simulating real-world fractional dynamical systems.

***Keywords*:** Riemann-Liouville (RL) fractional, Romanovski-Jacobi Polynomials (R-JPs), ψ-fractional diffusion equations

MSC: 34K37, 33C45, 35K57

1. Introduction

Fractional differential equations, an important part of mathematical modeling across diverse fields like physics [1], engineering [2], biology [3], and finance [4], rely on integer-order derivatives, reflecting the number of times a function is differentiated. However, numerous real-world systems exhibit intricate behaviors not fully captured by integer-order derivatives. Consequently, there is growing interest in incorporating fractional calculus, encompassing integrals and derivatives of non-integer order, into the classical framework of differential calculus. This extension proves particularly beneficial for modeling systems with unusual diffusion, effects of memory, and non-local interactions [5, 6]. Within this framework, fractional differential equations emerge as a powerful tool for describing such complex dynamics.

The fourth-order ψ-fractional sub-diffusion equation simulates complicated anomalous transport processes found in viscoelastic materials, porous media, and plasma turbulence. This model accurately captures non-Fickian transport

DOI: https://doi.org/10.37256/cm.7320267644

phenomena as well as super diffusive or sub-diffusive behavior by accounting for both nonlocal memory effects (via the ψ-fractional time derivative) and high-order spatial interactions (via the fourth-order derivative), unlike classical diffusion equations. The general form of the model is:

$$D^{\delta_1,\,\psi}\mathscr{Y}(\chi,\,\rho)+\frac{\partial^4\mathscr{Y}(\chi,\,\rho)}{\partial\chi^4}=\mathscr{F}(\chi,\,\rho,\,\mathscr{Y}(\chi,\,\rho)),\quad 0<\chi<1,\,\rho>0, \tag{1}$$

with the initial-Dirichlet boundary conditions

$$\begin{cases} \mathscr{Y}(0,\,\rho)=\psi_1(\rho), \qquad \mathscr{Y}(1,\,\rho)=\psi_2(\rho), \qquad \mathscr{Y}(\chi,\,0)=\psi_3(\chi), \\ \dfrac{\partial^2\mathscr{Y}(0,\,\rho)}{\partial\chi^2}=\psi_4(\rho), \qquad \dfrac{\partial^2\mathscr{Y}(1,\,\rho)}{\partial\chi^2}=\psi_5(\rho), \end{cases} \tag{2}$$

where $D^{\delta_1,\,\psi}\mathscr{Y}(\chi,\,\rho)$ is the ψ-fractional Caputo-type derivative of order $1<\delta_1<2$ $\mathscr{Y}(\chi,\,\rho)$ is the unknown physical quantity, such as temperature or concentration.

The ψ-fractional differential equation may simulate complicated systems with memory effects and hereditary features, making it frequently applicable in science and engineering. In physics, it describes anomalous diffusion processes and nonlocal phenomena in fractal-structured materials. In control theory, ψ-fractional models improve control system stability and resilience, especially in robotics and automation. These equations are used in biomedical sciences for modeling biological processes such as drug transport in tissues and brain signal transmission. The ψ-fractional differential equation offers a more adaptable solution for real-world applications when traditional derivatives are insufficient. The paper in [7] presents a stable and efficient numerical method for the time-fractional Black-Scholes equation used in option pricing. Using a finite-difference scheme with a local Radial Basis Function (RBF) partition of unity approach, while the paper in [8] develops two efficient numerical schemes-based on backward Euler and second-order Backward Differentiation Formula (BDF) methods-for solving generalized tempered integro-differential equations with respect to another function. The authors in [9] present an accurate and efficient algorithm for the 3D nonlocal heat equation with a weakly singular kernel, combining a nonuniform-mesh Crank-Nicolson time discretization with a Galerkin finite element spatial scheme and an Alternating Direction Implicit (ADI) strategy to reduce computational cost.

In [10], the author utilized a ψ-Haar wavelet operational matrix to solve ψ Riccati fractional differential equations, whereas [11] addresses several theorems related to the ψ variable order. In [12], the authors solved ψ-Caputo time-fractional systems by applying the Laplace transform, fixed-point theory, and Grönwall's inequality. Similarly, [13] introduced the ψ-Caputo fractional derivative approach for solving fractional partial differential equations using the ψ-Haar wavelet operational matrix. Furthermore, Zhao et al. [14] applied the mapped Jacobi function together with ψ-fractional differential equations and the Petrov-Galerkin spectral method to problems involving boundary and initial conditions.

Spectral methods [15, 16] employ orthogonal basis functions to deliver precise approximations having high convergence rates. Orthogonal basis functions, utilized in spectral approaches [16], provide precise approximations with high convergence rates. Meshless approaches [17, 18], such as Method of Fundamental Solutions (MFS) and RBF interpolation, are effective for complex boundary conditions and irregular geometries. These methods contribute to a better understanding of memory effects, anomalous diffusion. For four decades, spectral methods have been widely applied across various fields, as highlighted in [19–22]. Initially, Fourier-based spectral methods were restricted to specific cases, such as periodic boundary conditions and simple geometries. However, recent theoretical advancements have significantly expanded their applicability, enabling effective solutions to a wide range of problems. Compared to other numerical methods, spectral approaches offer superior accuracy and exponential convergence rates. These methods represent solutions as finite series of orthogonal functions. Several spectral techniques exist, including collocation [23–26], tau [27–29], Galerkin [30], and Petrov-Galerkin [31], where coefficients are optimized to minimize absolute errors. For instance,

spectral collocation approximates differential equation solutions with remarkable accuracy, allowing residuals to approach zero at specific points.

The main goal of this article is to utilize the Romanovski-Jacobi Spectral Collocation (RJSC) method to approximate Fourth-Order ψ-Fractional Sub-Diffusion models (FO-ψFSDEs). To approach the numerical solution, the problem's residuals are calculated using a finite expansion. When initial and boundary criteria are enforced, the approach produces more accurate numerical outputs that are reliable and consistent.

In this work, we develop a novel RJSC method for the numerical solution of fourth-order ψ-fractional sub-diffusion equations. The proposed scheme leverages the orthogonality and adaptability of Romanovski-Jacobi Polynomials (R-JPs) to efficiently approximate both the spatial derivatives and ψ-fractional operators, leading to high accuracy with relatively few collocation points. Unlike classical spectral approaches that rely solely on Jacobi or Legendre bases, the use of Romanovski-Jacobi functions provides enhanced flexibility for handling non-standard kernels and boundary behaviors arising in ψ-fractional models. The effectiveness and robustness of the method are demonstrated through several benchmark examples, confirming its superiority in accuracy and convergence. Therefore, the proposed RJSC framework offers a powerful and efficient numerical tool for modeling complex anomalous diffusion processes governed by ψ-fractional dynamics.

The remainder of this manuscript is organized as follows. In Section 2, we present essential preliminaries and mathematical concepts related to ψ-fractional calculus and the Romanovski-Jacobi polynomial basis. Section 3 introduces the proposed Romanovski-Jacobi spectral collocation scheme and details the construction of the numerical method. In Section 4, several numerical examples are provided to illustrate the accuracy, efficiency, and convergence behavior of the developed approach. Finally, Section 5 summarizes the main conclusions and outlines potential directions for future research.

2. Fundamental concepts

In this section, we introduce key definitions and lemmas that will be utilized during the remainder of this work.

2.1 *Fractional calculus*

This section specifies the fundamental terms used throughout the subsequent sections.

Definition 1 [32] The right and left Caputo fractional derivative D^{α_1} of order α_1 are

$$D_{+}^{\alpha_1}\mathscr{Y}(\theta)=\frac{1}{\Gamma(\eta-\alpha_1)}\left(\int_0^{\theta}(\theta-\kappa)^{\eta-\alpha_1-1}\mathscr{Y}^{(\eta)}(\kappa)d\kappa\right),\quad \eta-1<\alpha_1\leq\eta,\ \theta>0. \tag{3}$$

$$D_{-}^{\alpha_1}\mathscr{Y}(\theta)=\frac{(-1)^{\eta}}{\Gamma(\eta-\alpha_1)}\left(\int_{\theta}^{L}(\kappa-\theta)^{\eta-\alpha_1-1}\mathscr{Y}^{(\eta)}(\kappa)d\kappa\right),\quad \eta-1<\alpha_1\leq\eta,\ \theta>0. \tag{4}$$

The operator $D_{\pm}^{\alpha_1}$ has the subsequent property:

$$D_{\pm}^{\alpha_1}I_{\pm}^{\alpha_1}\mathscr{Y}(\kappa)=I_{\pm}^{\alpha_1}D_{\pm}^{\alpha_1}\mathscr{Y}(\kappa)=-\sum_{\omega_1=0}^{\lceil\alpha_1\rceil-1}\mathscr{Y}^{(\omega_1)}(0^{+})\frac{\kappa^{\omega_1}}{\omega_1!}+\mathscr{Y}(\kappa), \tag{5}$$

$D^{\alpha_1}\pm$ and $I\pm^{\alpha_1}$ represent the operator values for both the left and right Caputo derivatives and integrals, respectively.

Definition 2 [32] For the Riemann-Liouville fractional integrals with order $\alpha_1>0$, the right- and left-sided formulations are:

$$I_{+}^{\alpha_1}\mathscr{Y}(\sigma_1) = \frac{1}{\Gamma(\alpha_1)}\int_0^{\sigma_1}(\sigma_1-\kappa)^{\alpha_1-1}\mathscr{Y}(\kappa)d\kappa, \tag{6}$$

$$I_{-}^{\alpha_1}\mathscr{Y}(\sigma_1) = \frac{1}{\Gamma(\alpha_1)}\int_{\sigma_1}^{L}(m-\sigma_1)^{\alpha_1-1}\mathscr{Y}(m)dm. \tag{7}$$

2.2 *The ψ fractional calculus*

This section outlines essential concepts, definitions, and results from ψ-fractional calculus that will be utilized in the following sections. For $p \geq 1$, the space $L_p^{\psi}(c,\ d)$, denotes the set of Lebesgue measurable functions on the finite interval $(c,\ d)$ that are p-integrable with respect to the measure $d\psi$:

$$L_{\psi}^{p}(c,\ d) := \left[\mathscr{Y} : \int_c^d |\hat{\mathscr{U}}(\chi)|^p d\psi < \infty\right].$$

$L_{\psi}^{p}(c,\ d)$ is a Banach space with norm $||\mathscr{Y}||_{L_{\psi}^{p}}$,

$$||\mathscr{Y}||_{L_{\psi}^{p}} = \left(\int_c^d |(\hat{\chi})|^p d\psi\right)^{1/p}.$$

When $p = 2$, space $L_{\psi}^{p}(c,\ d)$ transforms into a Hilbert space with inner product:

$$(\mathscr{Y},\ \hat{\mathscr{V}})_{\psi} = \int_c^d \mathscr{Y}(\chi)\hat{\mathscr{V}}(\chi)d\psi.$$

We utilize $L_{\psi}^{2}(c,\ d)$ for weighted Hilbert space with inner product:

$$(\mathscr{Y},\ \hat{\mathscr{V}})_{\Omega} = \int_c^d \mathscr{Y}(\chi)\hat{\mathscr{V}}(\chi)\Omega(\chi)d\chi.$$

Definition 3 [33, 34] The left- and right-sided ψ-fractional integrals of a function $\mathscr{Y}(\chi)$ with order $\alpha_1 > 0$ are defined as

$${}_{\psi}D_{c,\ \chi}^{-\alpha_1} = \frac{1}{\Gamma(\alpha_1)}\int_c^{\chi}\psi'(\rho)\big(\psi(\chi)-\psi(\rho)\big)\big)^{\alpha_1-1}\mathscr{Y}(\rho)d\rho, \quad \chi \in (c,\ d),$$

$${}_{\psi}D_{\chi,\ d}^{-\alpha_1} = \frac{1}{\Gamma(\alpha_1)}\int_{\chi}^{d}\psi'(\rho)\big(\psi(\rho)-\psi(\chi)\big)\big)^{\alpha_1-1}\mathscr{Y}(\rho)d\rho, \quad \chi \in (c,\ d).$$

In the preceding formulation, the condition $\mathscr{Y}(\chi) \in L_{\psi}^{1}(c,\ d)$ is frequently assumed to be necessary but applicable. The options of ψ in the preceding definition are as follows.

Remark 1 Definition 3 defines fractional operators ${}_{\psi}D_{c,\chi}^{-\alpha_1}$ and ${}_{\psi}D_{\chi,d}^{-\alpha_1}$, which generalize existing fractional integral operators:

- $\psi(\chi)=\chi$ is the classical Riemann-Liouville-type fractional integral.
- $\psi(\chi)=log(\chi)$ is the Hadamard fractional integral [35–37].
- $\psi(\chi)=exp(\chi)$ is the fractional integral with exponential kernel [38].

Lemma 1 [34] The semigroup property described below is applicable: for $\alpha_1,\ \beta_1>0,\ \alpha_1+\beta_1>0$

$$ {}_{\psi}D_{c,\chi}^{-\alpha_1}\left({}_{\psi}D_{c,\chi}^{-\beta_1}\mathscr{Y}(\chi)\right)={}_{\psi}D_{c,\chi}^{-(\alpha_1+\beta_1)}\mathscr{Y}(\chi),\qquad {}_{\psi}D_{\chi,d}^{-\alpha_1}\left({}_{\psi}D_{\chi,d}^{-\beta_1}\mathscr{Y}(\chi)\right)={}_{\psi}D_{\chi,d}^{-(\alpha_1+\beta_1)}\mathscr{Y}(\chi). $$

Lemma 2 [33, 39] The findings below are applicable for $\alpha_1>0,\ \beta_1>-1$

$$ {}_{\psi}D_{c,\chi}^{-\alpha_1}\big(\psi(\chi)-\psi(c)\big)^{\nu}=\frac{\Gamma(\nu+1)}{\Gamma(\nu+\alpha_1+1)}\big(\psi(\chi)-\psi(c)\big)^{\nu+\alpha_1}, $$

$$ {}_{\psi}D_{\chi,d}^{-\alpha_1}\big(\psi(d)-\psi(\chi)\big)^{\nu}=\frac{\Gamma(\nu+1)}{\Gamma(\nu+\alpha_1+1)}\big(\psi(d)-\psi(\chi)\big)^{\mu+\alpha_1}. $$

Definition 4 [34] For $\chi\in(c,\ d)$, the left- and right-sided ψ-Riemann-Liouville fractional derivatives (also known as ψ-derivatives) of a given function $\mathscr{Y}(\chi)$ with order $\alpha_1>0$ are defined as

$$ {}_{\psi}D_{c,\chi}^{-\alpha_1}\mathscr{Y}(\chi)=\delta_{\psi}^{n}\left[{}_{\psi}D_{c,\chi}^{-(n-\alpha_1)}\mathscr{Y}(\chi)\right]=\frac{1}{\Gamma(n-\alpha_1)}\delta_{\psi}^{n}\int_{c}^{\chi}\psi'(\rho)\big(\psi(\chi)-\psi(\rho)\big)^{n-\alpha_1-1}\mathscr{Y}(\rho)d\rho, $$

$$ {}_{\psi}D_{\chi,d}^{-\alpha_1}\mathscr{Y}(\chi)=(-1)^{n}\delta_{\psi}^{n}\left[{}_{\psi}D_{\chi,d}^{-(n-\alpha_1)}\mathscr{Y}(\chi)\right]=\frac{(-1)^{n})}{\Gamma(n-\alpha_1)}\delta_{\psi}^{n}\int_{\chi}^{d}\psi'(\rho)\big(\psi(\rho)-\psi(\chi)\big)^{n-\alpha_1-1}\mathscr{Y}(\rho)d\rho. $$

Definition 5 [34] For $\chi\in(c,\ d)$, the left-sided and right-sided ψ-Caputo fractional derivatives of a known function $\mathscr{Y}(\chi)$ with order$\alpha_1\in(n-1,\ n),\ n\in N+$ are defined as:

$$ {}_{C}\psi D_{c,\chi}^{\alpha_1}\mathscr{Y}(\chi)={}_{\psi}D_{c,\chi}^{-(n-\alpha_1)}\left[\delta_{\psi}^{n}\mathscr{Y}(\chi)\right]=\frac{1}{\Gamma(n-\alpha_1)}\int_{c}^{\chi}\psi'(\rho)\big(\psi(\chi)-\psi(\rho)\big)^{n-\alpha_1-1}\delta_{\psi}^{n}\mathscr{Y}(\rho)d\rho, $$

$$ {}_{C}\psi D_{\chi,d}^{\alpha_1}\mathscr{Y}(\chi)=(-1)_{\psi}^{n}D_{\chi,d}^{-(n-\alpha_1)}\left[\delta_{\psi}^{n}\mathscr{Y}(\chi)\right]=\frac{(-1)^{n}}{\Gamma(n-\alpha_1)}\int_{\chi}^{d}\psi'(\rho)\big(\psi(\rho)-\psi(\chi)\big)^{n-\alpha_1-1}\delta_{\psi}^{n}\mathscr{Y}(\rho)d\rho. $$

2.3 *The R-J polynomials*

RJSC techniques are extremely successful for solving Distributed-Order Fractional Complex Differential Equations (DOFCDEs) because of their ability to scale and responsiveness to variable modifications, particularly those using Jacobi polynomials. These approaches efficiently address issues that grow in size or complexity while retaining performance as approximation accuracy increases with additional points of collocation. They are capable of analyzing DOFCDEs at numerous levels, ranging from localized dynamics to large systems, while maintaining computational effectiveness. These techniques' efficiency in terms of Jacobi polynomial parametric variance originates from its durability and adaptability for utilize with different forms of fractional differential equations with changing variables. Scientists can improve both the

convergence rate and correctness of computational solutions by continually modifying Jacobi polynomial variables, hence increasing the method's overall effectiveness.

Definition 6 [40] The Romanovski Polynomials (RPs) with degree i and of form $(\rho_1,\ \sigma_1)$ indicate with $\hat{\mathscr{R}}_{\ell}^{(\rho_1,\ \sigma_1)}$ and are defined

$$\hat{\mathscr{R}}_{\ell}^{(\rho_1,\ \sigma_1)} := \frac{(\rho_1+1)_{\ell}}{\ell!}\,{}_2F_1(-\ell,\ \ell+\rho_1+\sigma_1+1;\ \rho_1+1,\ \rho). \tag{8}$$

Using the provided values $\rho_1 > -1$ and $\sigma_1 < -2\mathscr{M} - \rho_1 - 1$, the explicit equation following may be utilized for generating the collocation comprising $(\mathscr{M}+1)$ amount of the one dimensional R-JPs on $[0,\ \infty)$.

$$\hat{\mathscr{R}}_{\ell}^{(\rho_1,\ \sigma_1)}(\rho) = \sum_{k=0}^{\ell} \frac{(-1)^k\,(\Gamma(\ell+\rho_1+1)\Gamma(-\ell-\rho_1-\sigma_1))}{k!\Gamma(\ell-k+1)\Gamma(k+\rho_1+1)\Gamma(-\ell-k-\rho_1-\sigma_1)}\rho^k,\ \ell = 0,\ ...,\ \mathscr{M}. \tag{9}$$

On the range $[0,\ \infty]$, the R-JPs, given as $\hat{\mathscr{R}}_{\ell}^{(\rho_1,\ \sigma_1)}(\rho)$, are orthogonal with regard to the weight function $W(\rho) = \rho^{\rho_1}(1+\chi)^{\sigma_1}$. Their criteria for orthogonality is as follows:

$$\int_0^{\infty} \hat{\mathscr{R}}_{n}^{(\rho_1,\ \sigma_1)}(\chi)\hat{\mathscr{R}}_{m}^{(\rho_1,\ \sigma_1)}(\chi)w(\chi)\,d\chi = h_n\delta_{nm},$$

where $h_{\ell} = \dfrac{\Gamma(\ell+\rho_1+1)\Gamma(-\ell-\rho_1-\sigma_1)}{\Gamma(2\ell+\rho_1+\sigma_1+1)\ell!\Gamma(-\ell-\sigma_1)}$ is a normalization constant.

Theorem 3 Consider $\rho_1 > -1$ and $\rho_1+\sigma_1+N+1 < 0$. For $0 \le \ell,\ m \le \dfrac{N}{2}$, the RPs [40]

$$\int_0^{\infty} \hat{\mathscr{R}}_{\ell}^{(\rho_1,\ \sigma_1)}(\rho)\hat{\mathscr{R}}_{m}^{(\rho_1,\ \sigma_1)}(\rho)w_{\rho_1,\ \sigma_1}(\rho)\,dt = (-1)^{\ell+1}\frac{\Gamma(-\ell-\rho_1-\sigma_1)\Gamma(\ell+\rho_1+1)(\sigma_1+1)_{\ell}}{\ell!(2\ell+\rho_1+\sigma_1+1)\Gamma(-\sigma_1)}\delta_{\ell m}, \tag{10}$$

where the weight function is $w_{\rho_1,\ \sigma_1}(\rho) = \rho^{\rho_1}(1+\rho)^{\sigma_1}$.

The relation between the Jacobi $\hat{\mathscr{J}}_{\ell}^{(\rho_1,\ \sigma_1)}(\rho)$ and the RPs $\hat{\mathscr{R}}_{\ell}^{(\rho_1,\ \sigma_1)}(\rho)$ is given by

$$\hat{\mathscr{R}}_{\ell}^{(\rho_1,\ \sigma_1)}(\rho) = \hat{\mathscr{J}}_{\ell}^{(\rho_1,\ \sigma_1)}(1+2\rho), \tag{11}$$

the explicit description of RPs is expressed via

$$\hat{\mathscr{R}}_{\ell}^{(\rho_1,\ \sigma_1)}(\rho) := \sum_{m=0}^{\ell} a_{\ell,\ m}^{(\rho_1,\ \sigma_1)}\rho^m, \quad a_{\ell,\ m}^{(\rho_1,\ \sigma_1)} = \begin{pmatrix} \ell+\rho_1+\sigma_1+m \\ m \end{pmatrix}\begin{pmatrix} \ell+\rho_1 \\ \ell-m \end{pmatrix}. \tag{12}$$

R-JPs are eigenfunctions of the Sturm-Liouville operator $\mathscr{L}_{\rho_1,\ \sigma_1}$ is defined as:

$$\begin{aligned}\mathscr{L}_{\rho_1,\,\sigma_1}u &:= \rho(1+\rho)\partial_\rho^2 u(\rho)+((2+\rho_1+\sigma_1)\rho+(1+\rho_1))\partial_\rho u(\rho)\\ &= \rho^{-\rho_1}(1+\rho)^{-\sigma_1}\partial_\rho(\rho^{\rho_1+1}(1+\rho)^{\rho_1+1}\partial_\rho u(\rho)).\end{aligned} \tag{13}$$

Lemma 4 The following recursive relationship applies to the one-dimensional R-JPs [41]

$$\begin{cases}\hat{\mathscr{R}}_{\ell+1}^{(\rho_1,\,\sigma_1)}(\rho)=\big(A_\ell^{(\rho_1,\,\sigma_1)}(\rho)-B_\ell^{(\rho_1,\,\sigma_1)}\big)\hat{\mathscr{R}}_\ell^{(\rho_1,\,\sigma_1)}(\rho)-C_\ell^{(\rho_1,\,\sigma_1)}\hat{\mathscr{R}}_{\ell-1}^{(\rho_1,\,\sigma_1)}(\rho), \quad \ell\le 1,\\ \hat{\mathscr{R}}_0^{(\rho_1,\,\sigma_1)}(\rho),\\ \hat{\mathscr{R}}_1^{(\rho_1,\,\sigma_1)}(\rho)=(\rho_1+\sigma_1+2)\rho+\rho_1+1,\end{cases} \tag{14}$$

where

$$\begin{cases}A_\ell^{(\rho_1,\,\sigma_1)}=\dfrac{(2\ell+\rho_1+\sigma_1+1)(2\ell+\rho_1+\sigma_1+2)}{(\ell+1)(\ell+\rho_1+\sigma_1+1)},\\ B_\ell^{(\rho_1,\,\sigma_1)}=-\dfrac{(2\ell+\rho_1+\sigma_1+1)(2\ell(\ell+1)+(\rho_1+\sigma_1)(\rho_1+2\ell+1))}{(\ell+1)(\ell+\rho_1+\sigma_1+1)(2\ell+\rho_1+\sigma_1)},\\ C_\ell^{(\rho_1,\,\sigma_1)}=\dfrac{(\ell+\rho_1)(\ell+\sigma_1)(2\ell+\rho_1+\sigma_1+2)}{(\ell+1)(\ell+\rho_1+\sigma_1+1)(2\ell+\rho_1+\sigma_1)}.\end{cases} \tag{15}$$

Theorem 5 The R-JPs satisfy [41]

$$\rho(\rho+1)\partial_\rho\hat{\mathscr{R}}_\ell^{\rho_1,\,\sigma_1}(\rho)=A_\ell^{\rho_1,\,\sigma_1}\hat{\mathscr{R}}_{\ell-1}^{\rho_1,\,\sigma_1}(\rho)+B_\ell^{\rho_1,\,\sigma_1}\hat{\mathscr{R}}_\ell^{\rho_1,\,\sigma_1}(\rho)+C_\ell^{\rho_1,\,\sigma_1}\hat{\mathscr{R}}_{\ell+1}^{\rho_1,\,\sigma_1}(\rho), \tag{16}$$

where

$$\begin{aligned}A_\ell^{\rho_1,\,\sigma_1}&=-\frac{(\ell+\rho_1)(\ell+\sigma_1)(\ell+\rho_1+\sigma_1+1)}{(2\ell+\rho_1+\sigma_1+1)(2\ell+\rho_1+\sigma_1)},\\ B_\ell^{\rho_1,\,\sigma_1}&=\frac{\ell(\sigma_1-\rho_1)(\ell+\rho_1+\sigma_1+1)}{(2\ell+\rho_1+\sigma_1)(2\ell+\rho_1+\sigma_1+2)},\\ C_\ell^{\rho_1,\,\sigma_1}&=\frac{\ell(\ell+1)(\ell+\rho_1+\sigma_1+1)}{(2\ell+\rho_1+\sigma_1+1)(2\ell+\rho_1+\sigma_1+2)}.\end{aligned} \tag{17}$$

Lemma 6 [42] The R-JPs are the eigenfunctions of the singular Sturm-Liouville issue:

$$\mathscr{L}_{\rho_1,\,\sigma_1}\hat{\mathscr{R}}_{\ell}^{\rho_1,\,\sigma_1}(\rho)=\delta_{\ell}^{\rho_1,\,\sigma_1}\hat{\mathscr{R}}_{\ell}^{\rho_1,\,\sigma_1}(\rho), \tag{18}$$

with their corresponding eigenvalues

$$\delta_{\ell}^{\rho_1,\,\sigma_1}=\ell(\ell+\rho_1+\sigma_1+1)<0. \tag{19}$$

Theorem 7 The R-JP derivatives are provided by [41]

$$\frac{d^q}{d\rho^q}\hat{\mathscr{R}}_{m}^{\rho_1,\,\sigma_1}(\rho)=\sum_{l=0}^{m-q}C_{l,\,m}^{\rho_1,\,\sigma_1,\,q}\hat{\mathscr{R}}_{l}^{\rho_1,\,\sigma_1}(\rho), \tag{20}$$

where

$$C_{l,\,m}^{\rho_1,\,\sigma_1,\,q}=\frac{(-1)^q\Gamma(-m-\rho_1-\sigma_1)}{\Gamma(-m-\rho_1-\sigma_1-q)}c_k^{n-q}(\rho_1+q,\,\sigma_1+q,\,\rho_1,\,\sigma_1). \tag{21}$$

Theorem 8 [42] (R-J-Gauss quatruture) R-J-Gauss nodes $\{\rho_\ell\}_{\ell=0}^{M}$ being the zeros of $\hat{\mathscr{R}}_{M+1}^{\rho_1,\,\sigma_1}$ and the corresponding weights are given by

$$\varpi_{\ell}^{\rho_1,\,\sigma_1}=\frac{G_M^{\rho_1,\,\sigma_1}}{\hat{\mathscr{R}}_{M}^{\rho_1,\,\sigma_1}(\rho_\ell)\partial_\rho\hat{\mathscr{R}}_{M+1}^{\rho_1,\,\sigma_1}(\rho_\ell)}=\frac{\check{G}_M^{\rho_1,\,\sigma_1}}{\rho_\ell(1+\rho_\ell)\left[\partial_\rho\hat{\mathscr{R}}_{M+1}^{\rho_1,\,\sigma_1}(\rho_\ell)\right]^2}, \tag{22}$$

where

$$\begin{aligned}G_M^{\rho_1,\,\sigma_1}&=\frac{(2M+\rho_1+\sigma_1+2)\Gamma(-M-\rho_1-\sigma_1-1)\Gamma(1+M+\rho_1)}{(M+1)!\Gamma(-M-\sigma_1)},\\ \check{G}_M^{\rho_1,\,\sigma_1}&=\frac{\Gamma(-M-\rho_1-\sigma_1-1)\Gamma(2+M+\rho_1)}{(M+1)!\Gamma(-M-\sigma_1-1)}.\end{aligned} \tag{23}$$

3. The spectral collocation method

In this section, we provide a technique for solving the FO-ψFSDEs by utilizing the RJSC methodology. This approach is described as follows:

$$D^{\delta_1,\,\psi}\mathscr{Y}(\chi,\,\rho)+\frac{\partial^4\mathscr{Y}(\chi,\,\rho)}{\partial\chi^4}=\mathscr{F}(\chi,\,\rho,\,\mathscr{Y}(\chi,\,\rho)),\quad 0<\chi<1,\,\rho>0, \tag{24}$$

with the initial-Dirichlet boundary conditions

$$\begin{cases} \mathscr{Y}(0,\,\rho)=\psi_1(\rho), \qquad \mathscr{Y}(1,\,\rho)=\psi_2(\rho), \qquad \mathscr{Y}(\chi,\,0)=\psi_3(\chi), \\ \dfrac{\partial^2\mathscr{Y}(0,\,\rho)}{\partial\chi^2}=\psi_4(\rho), \qquad \dfrac{\partial^2\mathscr{Y}(1,\,\rho)}{\partial\chi^2}=\psi_5(\rho). \end{cases} \tag{25}$$

The approximate solution of $\check{\mathscr{Y}}(\chi,\,\rho)$ can be extended by integrating the shifted Jacobi polynomials with the shifted R-JPs

$$\check{\mathscr{Y}}(\chi,\,\rho)=\sum_{\substack{\hat{s}=0,\,1,\,...,\,\mathscr{M}\\ \hat{\rho}=0,\,1,\,...,\,\mathscr{N}}}\varepsilon_{\hat{s},\,\hat{\rho}}\,\hat{\mathscr{J}}_{\hat{s}}^{\alpha_1,\,\beta_1}(\chi)\hat{\mathscr{R}}_{\hat{\rho}}^{\rho_1,\,\sigma_1,\,\varepsilon}(\rho), \tag{26}$$

while $\hat{\mathscr{J}}_{\hat{s}}^{\alpha_1,\,\beta_1}(\chi)$ is shifted Jacobi polynomials $\hat{\mathscr{R}}_{\hat{\rho}}^{\rho_1,\,\sigma_1,\,\varepsilon}(\rho)$ is fractional R-JPs. Next, the spatial derivatives are obtained as

$$\begin{aligned} \frac{\partial\check{\mathscr{Y}}(\chi,\,\rho)}{\partial\chi}&=\sum_{\substack{\hat{s}=0,\,1,\,...,\,\mathscr{M}\\ \hat{\rho}=0,\,1,\,...,\,\mathscr{N}}}\varepsilon_{\hat{s},\,\hat{\rho}}\,\hat{\mathscr{J}}_{\hat{s},\,1}^{\alpha_1,\,\beta_1}(\chi)\hat{\mathscr{R}}_{\hat{\rho}}^{\rho_1,\,\sigma_1,\,\varepsilon}(\rho),\\ \frac{\partial^2\check{\mathscr{Y}}(\chi,\,\rho)}{\partial\chi^2}&=\sum_{\substack{\hat{s}=0,\,1,\,...,\,\mathscr{M}\\ \hat{\rho}=0,\,1,\,...,\,\mathscr{N}}}\varepsilon_{\hat{s},\,\hat{\rho}}\,\hat{\mathscr{J}}_{\hat{s},\,2}^{\alpha_1,\,\beta_1}(\chi)\hat{\mathscr{R}}_{\hat{\rho}}^{\rho_1,\,\sigma_1,\,\varepsilon}(\rho),\\ \frac{\partial^4\check{\mathscr{Y}}(\chi,\,\rho)}{\partial\chi^4}&=\sum_{\substack{\hat{s}=0,\,1,\,...,\,\mathscr{M}\\ \hat{\rho}=0,\,1,\,...,\,\mathscr{N}}}\varepsilon_{\hat{s},\,\hat{\rho}}\,\hat{\mathscr{J}}_{\hat{s},\,4}^{\alpha_1,\,\beta_1}(\chi)\hat{\mathscr{R}}_{\hat{\rho}}^{\rho_1,\,\sigma_1,\,\varepsilon}(\rho). \end{aligned} \tag{27}$$

The ψ-RL fractional derivative $D^{\delta_1,\,\psi}\mathscr{Y}(\chi,\,\rho)$ at $1<\delta_1<2$ as follows

$$D^{\delta_1,\,\psi}\mathscr{Y}(\chi,\,\rho)=\left(\frac{1}{\psi'(\rho)}\frac{d}{d\rho}\right)^2\left[\frac{1}{\Gamma(2-\delta_1)}\int_0^t(\psi(\rho)-\psi(\rho))^{1-\delta_1}\mathscr{Y}(\chi,\,\rho)d\rho\right] \tag{28}$$

Additionally, $D^{\delta_1,\,\psi}\check{\mathscr{Y}}(\chi,\,\rho)$, has been provided by utilize (28)

$$\begin{aligned} D^{\delta_1,\,\psi}\check{\mathscr{Y}}(\chi,\,\rho)&=\sum_{\substack{\hat{s}=0,\,1,\,...,\,\mathscr{M}\\ \hat{\rho}=0,\,1,\,...,\,\mathscr{N}}}\varepsilon_{\hat{s},\,\hat{\rho}}\,\hat{\mathscr{J}}_{\hat{s}}^{\alpha_1,\,\beta_1}(\chi)D^{\delta_1,\,\psi}(\hat{\mathscr{R}}_{\hat{\rho}}^{\rho_1,\,\sigma_1,\,\varepsilon}(\rho))\\ &=\sum_{\substack{\hat{s}=0,\,1,\,...,\,\mathscr{M}\\ \hat{\rho}=0,\,1,\,...,\,\mathscr{N}}}\varepsilon_{\hat{s},\,\hat{\rho}}\,\hat{\mathscr{J}}_{\hat{s}}^{\alpha_1,\,\beta_1}(\chi)\hat{\mathscr{R}}_{\hat{\rho},\,\delta_1,\,\psi}^{\rho_1,\,\sigma_1,\,\varepsilon}(\rho). \end{aligned} \tag{29}$$

Combing Eqs. (24)-(29), we obtain

$$\sum_{\substack{\hat{s}=0,\,1,\,...,\,\mathscr{M}\\ \hat{\rho}=0,\,1,\,...,\,\mathscr{N}}} \varepsilon_{\hat{s},\,\hat{\rho}}\,\hat{\mathscr{J}}_{\hat{s}}^{\alpha_1,\,\beta_1}(\chi)\hat{\mathscr{R}}_{\hat{\rho},\,\delta_1,\,\psi}^{\rho_1,\,\sigma_1,\,\varepsilon}(\rho)+\sum_{\substack{\hat{s}=0,\,1,\,...,\,\mathscr{M}\\ \hat{\rho}=0,\,1,\,...,\,\mathscr{N}}} \varepsilon_{\hat{s},\,\hat{\rho}}\,\hat{\mathscr{J}}_{\hat{s},\,4}^{\alpha_1,\,\beta_1}(\chi)\hat{\mathscr{R}}_{\hat{\rho}}^{\rho_1,\,\sigma_1,\,\varepsilon}(\rho)$$

$$=\mathscr{F}\left(\chi,\,\rho,\,\sum_{\substack{\hat{s}=0,\,1,\,...,\,\mathscr{M}\\ \hat{\rho}=0,\,1,\,...,\,\mathscr{N}}} \varepsilon_{\hat{s},\,\hat{\rho}}\,\hat{\mathscr{J}}_{\hat{s}}^{\alpha_1,\,\beta_1}(\chi)\hat{\mathscr{R}}_{\hat{\rho}}^{\rho_1,\,\sigma_1,\,\varepsilon}(\rho)\right). \tag{30}$$

Furthermore, the given conditions can be expressed as

$$\begin{cases} \sum\limits_{\substack{\hat{s}=0,\,1,\,...,\,\mathscr{M}\\ \hat{\rho}=0,\,1,\,...,\,\mathscr{N}}} \varepsilon_{\hat{s},\,\hat{\rho}}\,\hat{\mathscr{J}}_{\hat{s}}^{\alpha_1,\,\beta_1}(0)\hat{\mathscr{R}}_{\hat{\rho}}^{\rho_1,\,\sigma_1,\,\varepsilon}(\rho)=\psi_1(\rho), \\ \sum\limits_{\substack{\hat{s}=0,\,1,\,...,\,\mathscr{M}\\ \hat{\rho}=0,\,1,\,...,\,\mathscr{N}}} \varepsilon_{\hat{s},\,\hat{\rho}}\,\hat{\mathscr{J}}_{\hat{s}}^{\alpha_1,\,\beta_1}(1)\hat{\mathscr{R}}_{\hat{\rho}}^{\rho_1,\,\sigma_1,\,\varepsilon}(\rho)=\psi_2(\rho), \\ \sum\limits_{\substack{\hat{s}=0,\,1,\,...,\,\mathscr{M}\\ \hat{\rho}=0,\,1,\,...,\,\mathscr{N}}} \varepsilon_{\hat{s},\,\hat{\rho}}\,\hat{\mathscr{J}}_{\hat{s}}^{\alpha_1,\,\beta_1}(\chi)\hat{\mathscr{R}}_{\hat{\rho}}^{\rho_1,\,\sigma_1,\,\varepsilon}(0)=\psi_3(\chi), \\ \sum\limits_{\substack{\hat{s}=0,\,1,\,...,\,\mathscr{M}\\ \hat{\rho}=0,\,1,\,...,\,\mathscr{N}}} \varepsilon_{\hat{s},\,\hat{\rho}}\,\hat{\mathscr{J}}_{\hat{s},\,2}^{\alpha_1,\,\beta_1}(0)\hat{\mathscr{R}}_{\hat{\rho}}^{\rho_1,\,\sigma_1,\,\varepsilon}(\rho)=\psi_4(\rho), \\ \sum\limits_{\substack{\hat{s}=0,\,1,\,...,\,\mathscr{M}\\ \hat{\rho}=0,\,1,\,...,\,\mathscr{N}}} \varepsilon_{\hat{s},\,\hat{\rho}}\,\hat{\mathscr{J}}_{\hat{s},\,2}^{\alpha_1,\,\beta_1}(1)\hat{\mathscr{R}}_{\hat{\rho}}^{\rho_1,\,\sigma_1,\,\varepsilon}(\rho)=\psi_5(\rho). \end{cases} \tag{31}$$

The Equations (30) and (31) are nearest to being zero at specific nodes.

$$\begin{cases} \sum_{\substack{\hat{s}=0,\,1,\,...,\,\mathscr{M}\\ \hat{\rho}=0,\,1,\,...,\,\mathscr{N}}} \varepsilon_{\hat{s},\,\hat{\rho}}\,\hat{\mathscr{J}}_{\hat{s}}^{\alpha_1,\,\beta_1}\left(\chi_{\mathscr{M},\,\iota}^{\alpha_1,\,\beta_1}\right)\hat{\mathscr{R}}_{\hat{\rho},\,\delta_1,\,\psi}^{\rho_1,\,\sigma_1,\,\varepsilon}\left(\rho_{\kappa}^{\rho_1,\,\sigma_1,\,\varepsilon}\right) \\ +\sum_{\substack{\hat{s}=0,\,1,\,...,\,\mathscr{M}\\ \hat{\rho}=0,\,1,\,...,\,\mathscr{N}}} \varepsilon_{\hat{s},\,\hat{\rho}}\,\hat{\mathscr{J}}_{\hat{s},\,4}^{\alpha_1,\,\beta_1}\left(\chi_{\mathscr{M},\iota}^{\alpha_1,\,\beta_1}\right)\hat{\mathscr{R}}_{\hat{\rho}}^{\rho_1,\,\sigma_1\,,\varepsilon}(\rho_{\kappa}^{\rho_1,\,\sigma_1,\,\varepsilon}) \\ =\ \mathscr{F}\left(\chi_{\mathscr{M},\,\iota}^{\alpha_1,\,\beta_1},\,\rho_{\kappa}^{\rho_1,\,\sigma_1,\,\varepsilon},\,\sum_{\substack{\hat{s}=0,\,1,\,...,\,\mathscr{M}\\ \hat{\rho}=0,\,1,\,...,\,\mathscr{N}}} \varepsilon_{\hat{s},\,\hat{\rho}}\,\hat{\mathscr{J}}_{\hat{s}}^{\alpha_1,\,\beta_1}\left(\chi_{\mathscr{M},\,\iota}^{\alpha_1,\,\beta_1}\right)\hat{\mathscr{R}}_{\hat{\rho}}^{\rho_1,\,\sigma_1,\,\varepsilon}\left(\rho_{\kappa}^{\rho_1,\,\sigma_1,\,\varepsilon}\right)\right), \\ \sum_{\substack{\hat{s}=0,\,1,\,...,\,\mathscr{M}\\ \hat{\rho}=0,\,1,\,...,\,\mathscr{N}}} \varepsilon_{\hat{s},\,\hat{\rho}}\,\hat{\mathscr{J}}_{\hat{s}}^{\alpha_1,\,\beta_1}(0)\hat{\mathscr{R}}_{\hat{\rho}}^{\rho_1,\,\sigma_1,\,\varepsilon}(\rho_{\kappa}^{\rho_1,\,\sigma_1,\,\varepsilon})=\psi_1(\rho_{\kappa}^{\rho_1,\,\sigma_1,\,\varepsilon}), \\ \sum_{\substack{\hat{s}=0,\,1,\,...,\,\mathscr{M}\\ \hat{\rho}=0,\,1,\,...,\,\mathscr{N}}} \varepsilon_{\hat{s},\,\hat{\rho}}\,\hat{\mathscr{J}}_{\hat{s}}^{\alpha_1,\,\beta_1}(1)\hat{\mathscr{R}}_{\hat{\rho}}^{\rho_1,\,\sigma_1,\,\varepsilon}(\rho_{\kappa}^{\rho_1,\,\sigma_1,\,\varepsilon})=\psi_2(\rho_{\kappa}^{\rho_1,\,\sigma_1,\,\varepsilon}), \\ \sum_{\substack{\hat{s}=0,\,1,\,...,\,\mathscr{M}\\ \hat{\rho}=0,\,1,\,...,\,\mathscr{N}}} \varepsilon_{\hat{s},\,\hat{\rho}}\,\hat{\mathscr{J}}_{\hat{s}}^{\alpha_1,\,\beta_1}\left(\chi_{\mathscr{M},\,\iota}^{\alpha_1,\,\beta_1}\right)\hat{\mathscr{R}}_{\hat{\rho}}^{\rho_1,\,\sigma_1,\,\varepsilon}(0)=\psi_3(\chi_{\mathscr{M},\,\iota}^{\alpha_1,\,\beta_1}), \\ \sum_{\substack{\hat{s}=0,\,1,\,...,\,\mathscr{M}\\ \hat{\rho}=0,\,1,\,...,\,\mathscr{N}}} \varepsilon_{\hat{s},\,\hat{\rho}}\,\hat{\mathscr{J}}_{\hat{s},\,2}^{\alpha_1,\,\beta_1}(0)\hat{\mathscr{R}}_{\hat{\rho}}^{\rho_1,\,\sigma_1,\,\varepsilon}(\rho_{\kappa}^{\rho_1,\,\sigma_1,\,\varepsilon})=\psi_5(\rho_{\kappa}^{\rho_1,\,\sigma_1,\,\varepsilon}), \\ \sum_{\substack{\hat{s}=0,\,1,\,...,\,\mathscr{M}\\ \hat{\rho}=0,\,1,\,...,\,\mathscr{N}}} \varepsilon_{\hat{s},\,\hat{\rho}}\,\hat{\mathscr{J}}_{\hat{s},\,2}^{\alpha_1,\,\beta_1}(1)\hat{\mathscr{R}}_{\hat{\rho}}^{\rho_1,\,\sigma_1,\,\varepsilon}(\rho_{\kappa}^{\rho_1,\,\sigma_1,\,\varepsilon})=\psi_5(\rho_{\kappa}^{\rho_1,\,\sigma_1,\,\varepsilon}). \end{cases} \tag{32}$$

Finally, solving the system is straightforward, allowing $\mathscr{Y}(\chi,\,\rho)$ to be expressed in a closed form.

4. Numerical results

The efficacy and precision of the proposed approach are demonstrated through the examples, where the Absolute Error (AEs) refers to the disparity between the observed and predicted solution:

$$AEs(\chi,\ \rho) = |\mathscr{Y}(\chi,\ \rho) - \check{\mathscr{Y}}(\chi,\ \rho)|. \tag{33}$$

For the point $\chi,\ \rho$, the approximate and exact solutions are $\mathscr{Y}(\chi,\ \rho)$ and $\check{\mathscr{Y}}(\chi,\ \rho)$. The approach for determining the largest AEs (L_∞) and (L_2) is as described below:

$$L_\infty = \max\{AEs(\chi,\ \rho)\}. \tag{34}$$

All numerical simulations and computations in this study were performed on a computer with an Intel Core i7 processor. The algorithm code was run via MATHEMATICA version 12.2.

Example 1 We consider FO-ψFSDEs,

$$\begin{cases} D^{\delta_1,\ \psi}\mathscr{Y}(\chi,\ \rho) + \dfrac{\partial^4\mathscr{Y}(\chi,\ \rho)}{\partial\chi^4} + \mathscr{Y}(\chi,\ \rho)^2 = \mathscr{F}(\chi,\ \rho), \\ \mathscr{Y}(0,\ \rho) = 0, \qquad \mathscr{Y}(1,\ \rho) = \rho\sin[1], \qquad \mathscr{Y}(\chi,\ 0) = 0, \\ \dfrac{\partial^2\mathscr{Y}(0,\ \rho)}{\partial\chi^2} = 0, \qquad \dfrac{\partial^2\mathscr{Y}(1,\ \rho)}{\partial\chi^2} = -\rho\sin[1], \end{cases} \tag{35}$$

where $\mathscr{F}(\chi,\ \rho)$ is given from the exact solution $\mathscr{Y}(\chi,\ \rho) = \rho\sin(\chi)$, $\psi(\rho) = 0.2\rho^3$, and $\delta_1 = 1.3,\ 1.5$. We obtain L_∞ for different $\mathscr{M}$ and $\mathscr{N}$ values in Table 1 in this Example 1. Figure 1 shows the AEs for Example 1 where $\delta_1 = 1.3$ and $\delta_1 = 1.5$ respectively. The convergence decay of our technique is shown in Figure 2. The results show that even by a few points our technique is more accurate. Taking $\delta_1 = 1.5$, and $\mathscr{N},\ \mathscr{M} = 4$, we obtain the numerical solution of Example 1 as:

$$\chi^3\rho[-0.082257 - 7.69189\times10^{-2}(-1+2\rho) + 5.98907\times10^{-3}(1-6\rho+6\rho^2)$$

$$-4.82563\times10^{-5}(-1+12\rho-30t^2+20\rho^3) - 6.99175\times10^{-4}(1-20\rho+90t^2-140\rho^3+70\rho^4)]$$

$$+\chi^2\rho[1.38778\times10^{-17} - 1.52222\times10^{-16}(1-6\rho+6\rho^2) - 4.22995\times10^{-16}(-1+12\rho-30\rho^{+}20\rho^3)$$

$$-2.88018\times10^{-16}(1-20\rho+90\rho^2-14\rho^3+70\rho^4)] + \rho[0. + 2.77556\times10^{-17}(-1+2\rho)$$

$$+1.33032\times10^{-16}(1-6\rho+6\rho^2) + 3.04903\times10^{-16}(-1+12\rho-30\rho^2+20\rho^3)$$

$$+2.07692\times10^{-16}(1-20\rho+90\rho^2-140\rho^3+70\rho^4)] + \chi\rho[4.96925\times10^{-1} + 4.94256\times10^{-1}(-1+2\rho)$$

$$-2.99454\times10^{-3}(1-6\rho+6\rho^2)+2.41281\times10^{-5}(-1+12\rho-30\rho^2+20\rho^3)$$

$$+3.49587\times10^{-4}(1-20\rho+90\rho^2-140\rho^3+70\rho^4)]+\chi^4\rho[6.06722\times10^{-3}+3.39814\times10^{-3}(-1+2\rho)$$

$$-2.99454\times10^{-3}(1-6\rho+6\rho^2)+2.41281\times10^{-5}(-1+12\rho-30\rho^2+20\rho^3)$$

$$+349587\times10^{-4}(1-20\rho+90\rho^2-140\rho^3+70\rho^4)]. \tag{36}$$

Table 1. The MAE for Example 1 with different values of $\mathcal{N}$, $\mathcal{M}$

$(\mathcal{N}, \mathcal{M})$	$\delta_1 = 1.3$	CPU (sec)	$\delta_1 = 1.5$	CPU (sec)
(4, 4)	3.465×10^{-3}	3.703	3.959×10^{-3}	3.999
(6, 6)	5.473×10^{-5}	4.702	5.810×10^{-5}	4.453
(8, 8)	2.303×10^{-7}	6.613	2.615×10^{-7}	6.374
(10, 10)	5.637×10^{-10}	13.548	5.539×10^{-10}	13.924

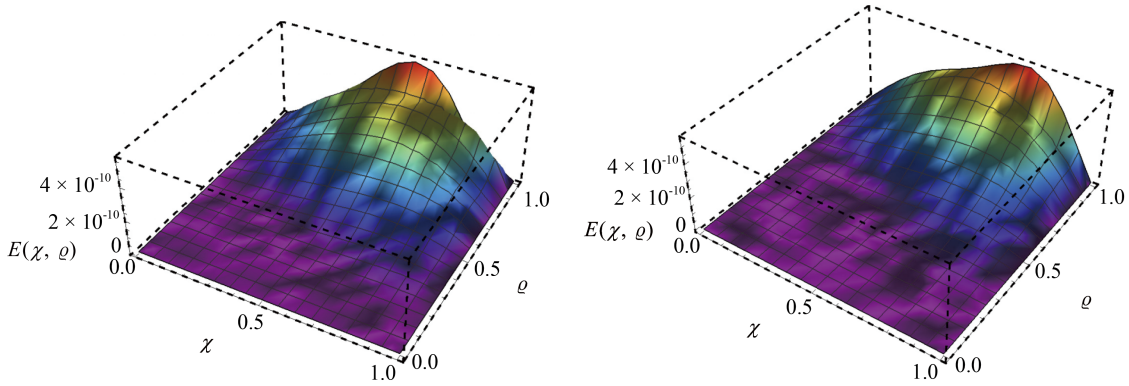

Figure 1. AEs for Example 1 for $N = M = 10$, and 1 = 1.3, 1.5 respectively

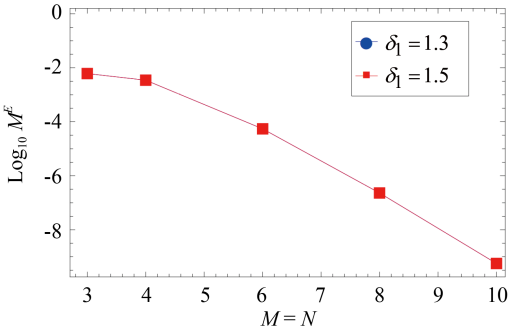

Figure 2. Mean Absolute Error (MAE) convergence for Example 1 for difference of M, N

Example 2 We consider FO-ψFSDEs,

$$\begin{cases} D^{\delta_1,\,\psi}\mathscr{Y}(\chi,\rho)+\dfrac{\partial^4\mathscr{Y}(\chi,\,\rho)}{\partial\chi^4}+\mathscr{Y}(\chi,\,\rho)^3=\mathscr{F}(\chi,\,\rho), \\ \mathscr{Y}(0,\,\rho)=\rho^3, \qquad \mathscr{Y}(1,\,\rho)=e^1\rho^3, \qquad \mathscr{Y}(\chi,\,0)=0, \\ \dfrac{\partial^2\mathscr{Y}(0,\,\rho)}{\partial\chi^2}=\rho^3, \qquad \dfrac{\partial^2\mathscr{Y}(1,\,\rho)}{\partial\chi^2}=e^1\rho^3, \end{cases} \tag{37}$$

where $\mathscr{F}(\chi,\,\rho)$ is given from the exact solution $\mathscr{Y}(\chi,\,\rho)=\rho^3e^{\chi}$, $\psi(\rho)=0.5\rho^2$, and $\delta_1=1.4,\,1.6,\,1.7$. We obtain L_∞ for different $\mathscr{M}$ and $\mathscr{N}$ values in Table 2 in this Example 2. Figure 3 shows the AEs for Example 2 where $\delta_1=1.4,\,1.6,\,1.7$ respectively. The convergence decay of our technique is shown in Figure 4. The results show that even by a few points our technique is more accurate. Taking $\delta_1=1.7$, and $\mathscr{N},\mathscr{M}=4$, we obtain the numerical solution of Example 2 as:

$$\begin{aligned} &\chi^3\rho[0.0453387+0.0830195(-1+2\rho)+0.0477077(1-6\rho+6\rho^2)+0.0098067(-1+12\rho-30\rho^2+20\rho^3) \\ &-0.0002203(1-20\rho+90\rho^2-140\rho^3+70\rho^4)]+\rho[0.25+0.45(-1+2\rho)+0.25(1-6\rho+6\rho^2) \\ &+0.05(-1+12\rho-30\rho^2+20\rho^3)-1.31605\times10^{-}16(1-20\rho+90\rho^2-140\rho^3+70\rho^4)] \\ &+\chi^2\rho[0.125+0.225(-1+2t)+0.125(1-6\rho+6\rho^2)+0.025(-1+12\rho-30\rho^2+20\rho^3) \\ &+1.62549\times10^{-}16(1.-20\rho+90\rho^2-140\rho^3+70\rho^4)]+\chi\rho[0.246104+0.442282(-1+2\rho) \\ &+0.244919(1-6\rho+6\rho^2)+0.0488512(-1+12\rho-30\rho^2+20\rho^3)+0.00011015(1-20\rho+90\rho^2-140\rho^3+70\rho^4)] \\ &+\chi^4\rho[0.0131282+0.0229258(-1+2\rho)+0.0119437(1-6\rho+6\rho^2)+0.00225616(-1+12\rho-30\rho^2+20\rho^3) \\ &+0.00011015(1-20\rho+90\rho^2-140\rho^3+70\rho^4)]. \end{aligned} \tag{38}$$

Table 2. The MAE for Example 2 with different values of $\mathscr{N}$, $\mathscr{M}$

$(\mathscr{N},\,\mathscr{M})$	$\delta_1=1.4$	CPU (sec)	$\delta_1=1.6$	CPU (sec)	$\delta_1=1.7$	CPU (sec)
(4, 4)	3.465×10^{-3}	3.361	3.959×10^{-3}	3.704	3.959×10^{-3}	3.859
(6, 6)	5.473×10^{-5}	4.046	5.810×10^{-5}	4.312	5.810×10^{-5}	4.687
(8, 8)	2.303×10^{-7}	6.515	2.615×10^{-7}	7.266	2.615×10^{-7}	7.187
(10, 10)	5.637×10^{-10}	15.079	5.539×10^{-10}	14.202	5.539×10^{-10}	14.859

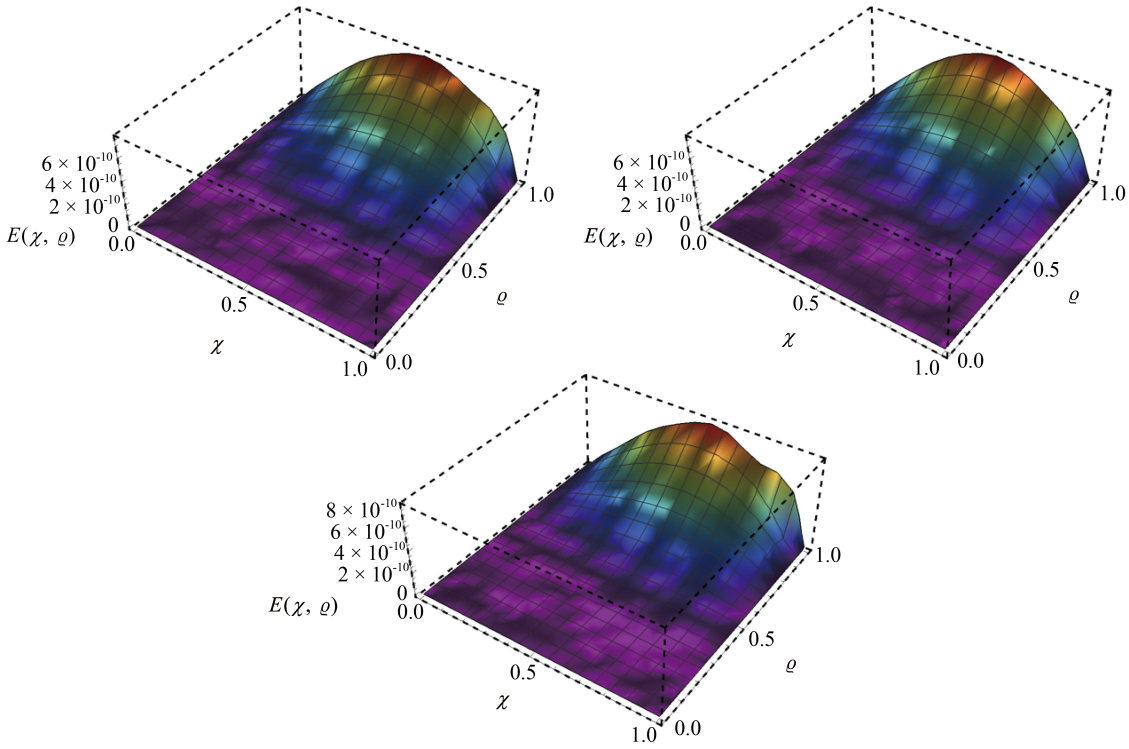

Figure 3. AEs for Example 2 for $N = M = 10$, and 1 = 1.4, 1.6, 1.7 respectively

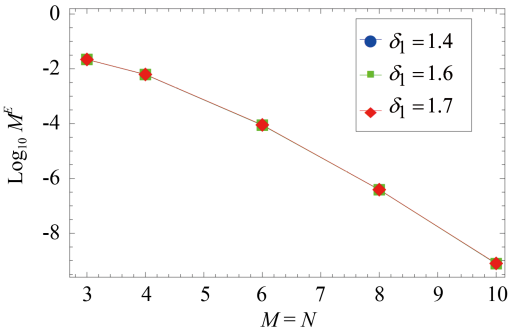

Figure 4. MAE convergence for Example 2 for difference of M, N

Example 3 We consider FO-ψFSDEs,

$$\begin{cases} D^{\delta_1,\,\psi}\mathscr{Y}(\chi,\,\rho)+\dfrac{\partial^4\mathscr{Y}(\chi,\,\rho)}{\partial\chi^4}+\mathscr{Y}(\chi,\,\rho)^2=\mathscr{F}(\chi,\,\rho), \\ \mathscr{Y}(0,\,\rho)=\rho^2, \qquad \mathscr{Y}(1,\,\rho)=\rho^2\cos[1], \qquad \mathscr{Y}(\chi,\,0)=0, \\ \dfrac{\partial^2\mathscr{Y}(0,\,\rho)}{\partial\chi^2}=-\rho^2, \qquad \dfrac{\partial^2\mathscr{Y}(1,\,\rho)}{\partial\chi^2}=-\rho^2\cos[1]. \end{cases} \tag{39}$$

In this example, the source term $\mathscr{F}(\chi, \rho)$ is constructed from the exact analytical solution $\mathscr{Y}(\chi, \rho) = \rho^2 \cos(\chi)$. We obtain L_∞ for different $\mathscr{M}$ and $\mathscr{N}$ values in Table 3 in this Example 3.

Table 3. The MAE for Example 3 with different values of $\mathscr{N}$, $\mathscr{M}$

$(\mathscr{N}, \mathscr{M})$	$\delta_1 = 1.5$	CPU (sec)	$\delta_1 = 1.9$	CPU (sec)
(4, 4)	1.56×10^{-3}	3.812	1.45×10^{-3}	3.421
(6, 6)	2.38×10^{-5}	4.0	0.184×10^{-5}	4.094
(8, 8)	1.04×10^{-7}	6.484	9.02×10^{-8}	6.189
(10, 10)	2.16×10^{-10}	13.842	2.13×10^{-10}	14.627

5. Conclusion

The paper introduces an accurate and efficient numerical approach to solve FO-ψFSDEs. To obtain spectral solutions, this technique utilized RJSC methods that take into account initial and boundary conditions. The approach achieves remarkable precision by computing quadrature points' residuals and converting them into algebraic systems. This innovation not only improves the precision of solving FO-ψFSDEs but also facilitates the exploration of complex systems governed by fractional dynamics in a variety of fields such as engineering, physics, and biology. The application of RJSC methods represents a significant advancement in numerical analysis, providing a solid foundation for addressing FO-ψFSDEs. The rigorous computing of residuals at quadrature points improves solution precision and ensures that the approach accurately depicts the system's underlying behavior. This degree of precision is required for areas involving technical design, scientific research, and risk management. The results demonstrate the accuracy and efficiency of this method through illustrative examples, confirming its potential for practical applications across physics, biology, and engineering. This work emphasizes the critical role of advanced numerical techniques in addressing fractional differential equations, paving the way for further research and advances in fractional modeling and computation.

Acknowledgment

This work of the last author (AB) was supported by Grambling State University for the Endowed Chair of Mathematics. The author thankfully acknowledges this support.

Conflict of interest

The authors declare that they have no competing interests.

References

[1] Bruce IH, Trevor AML, Peter S. An introduction to fractional diffusion. *Complex Physical, Biophysical and Econophysical Systems*. 2010; 37–89. Available from: https://doi.org/10.1142/9789814277327_0002.

[2] Anthony WL. *Systems of Nonlinear Partial Differential Equations: Applications to Biology and Engineering*. Vol. 49. Heidelberg: Springer Dordrecht; 2013.

[3] Jones DS, Plank MJ, Sleeman BD. Differential equations and mathematical biology. *International Journal Bioautomation*. 2011; 15(2): 140–143.

[4] Daniel S, Udeani CI. Multidimensional linear and nonlinear partial integro-differential equation in bessel potential spaces with applications in option pricing. *Mathematics*. 2021; 9(13): 1463.

[5] Tahereh E, Jalil R, Khosrow M. Existence, uniqueness, and approximate solutions for the general nonlinear distributed-order fractional differential equations in a banach space. *Advances in Difference Equations*. 2021; 2021(1): 461.
[6] Ahmed ZA, Mohamed AA, Emad S, Ibrahim AD. A spectral collocation method for solving the non-linear distributed-order fractional Bagley-Torvik differential equation. *Fractal and Fractional*. 2023; 7(11): 780.
[7] Omid N, Jalil R, Hossein J. Numerically pricing american and european options using a time fractional black-scholes model in financial decision-making. *Alexandria Engineering Journal*. 2025; 112: 235–245.
[8] Wenlin Q, Omid N, Zakieh A. Numerical investigation of generalized tempered type integrodifferential equations with respect to another function. *Fractional Calculus and Applied Analysis*. 2023; 26(6): 2580–2601.
[9] Luo M, Qiu WL, Nikan O, Avazzadeh Z. Second-order accurate, robust and efficient adi galerkin technique for the three-dimensional nonlocal heat model arising in viscoelas ticity. *Applied Mathematics and Computation*. 2023; 440: 127655.
[10] Ali A, Minamoto T. A new numerical technique for solving ψ-fractional riccati differential equations. *Journal of Applied Analysis & Computation*. 2023; 13(2): 1027–1043.
[11] Almeida R. On the variable-order fractional derivatives with respect to another function. *Aequationes Mathematicae*. 2024; 99: 805–822.
[12] Brahim BH, Fatima-Zahrae EA, Asmae T, Torres DFM. Existence and uniqueness of mild solutions for a class of psi-Caputo time-fractional systems of order from one to two: H. Ben Brahim et al. *Fractional Calculus and Applied Analysis*. 2025; 28(5): 2357–2394.
[13] Ali A, Minamoto T, Shah R, Nonlaopon K. A novel numerical method for solution of fractional partial differential equations involving the ψ-caputo fractional derivative. *AIMS Mathematics*. 2023; 8(1): 2137–2153.
[14] Zhao T, Zhao ZY, Li CP, Li DX. Spectral approximation of ψ-fractional differential equation based on mapped jacobi functions. *arXiv:2312.16426*. 2023. Available from: https://doi.org/10.48550/arXiv.2312.16426.
[15] Nouy A. Recent developments in spectral stochastic methods for the numerical solution of stochastic partial differential equations. *Archives of Computational Methods in Engineering*. 2009; 16(3): 251–285.
[16] Abdelkawy MA, Jeelani MB, Alnahdi AS, Taha TM, Soluma EM. Legendre spectral collocation method for distributed and riesz fractional convection-diffusion and Schrödinger-type equation. *Boundary Value Problems*. 2022; 2022(1): 1–15.
[17] Abbaszadeh M, Dehghan M. An improved meshless method for solving two dimensional distributed order time-fractional diffusion-wave equation with error estimate. *Numerical Algorithms*. 2017; 75: 173–211.
[18] Liu QZ, Mu SJ, Liu QX, Liu BQ, Bi XL, Zhuang PH, et al. An rbf based meshless method for the distributed order time fractional advection-diffusion equation. *Engineering Analysis with Boundary Elements*. 2018; 96: 55–63.
[19] Delzanno GL. Multi-dimensional, fully-implicit, spectral method for the Vlasov-Maxwell equations with exact conservation laws in discrete form. *Journal of Computational Physics*. 2015; 301: 338–356.
[20] Chen Y, Zhou J. Error estimates of spectral Legendre-Galerkin methods for the fourth-order equation in one dimension. *Applied Mathematics and Computation*. 2015; 268: 1217–1226.
[21] Abdelkawy MA, Amin AZM, Lopes AM. Fractional-order shifted Legendre collocation method for solving non-linear variable-order fractional Fredholm integro-differential equations. *Computational and Applied Mathematics*. 2022; 41(1): 1–21.
[22] Abd-Elhameed WM, Youssri YH. New formulas of the high-order derivatives of fifth-kind Chebyshev polynomials: Spectral solution of the convection-diffusion equation. *Numerical Methods for Partial Differential Equations*. 2024; 40(2): e22756.
[23] Amin A, Abdelkawy M, Amin A, Lopes AM, Alluhaybi A, Hashim I. Legendre-Gauss Lobatto collocation method for solving multi-dimensional systems of mixed Volterra-Fredholm integral equations. *AIMS Mathematics*. 2023; 8(9): 20871–20891.
[24] Tedjani AH, Amin AZ, Abdel-Aty AH, Abdelkawy MA, Mahmoud M. Legendre spectral collocation method for solving nonlinear fractional fredholm integro-differential equations with convergence analysis. *AIMS Mathematics*. 2024; 9(4): 7973–8000.
[25] Magdy E, Abd-Elhameed WM, Youssri YH, Moatimid GM, Atta AG. A potent collocation approach based on shifted gegenbauer polynomials for nonlinear time fractional Burgers' equations. *Contemporary Mathematics*. 2023; 4(4): 647–665.

[26] Amin AZ, Abdelkawy MA, Soluma EM, Babatin MM. A space-time spectral approximation for solving two dimensional variable-order fractional convection-diffusion equations with nonsmooth solutions. *International Journal of Modern Physics C*. 2024; 35: 2450088.
[27] Ezz-Eldien SS. On solving systems of multi-pantograph equations via spectral tau method. *Applied Mathematics and Computation*. 2018; 321: 63–73.
[28] Doha EH, Abdelkawy MA, Amin AZM, Baleanu D. Shifted jacobi spectral collocation method with convergence analysis for solving integro-differential equations and system of integro-differential equations. *Nonlinear Analysis: Modelling and Control*. 2019; 24(3): 332–352.
[29] Ahmed HM, Hafez RM, Abd-Elhameed WM. A computational strategy for nonlinear time-fractional generalized Kawahara equation using new eighth-kind Chebyshev operational matrices. *Physica Scripta*. 2024; 99(4): 045250.
[30] Youssri YH, Abd-Elhameed WM. Numerical spectral Legendre-Galerkin algorithm for solving time fractional telegraph equation. *Romanian Journal of Physics*. 2018; 63(107): 1–16.
[31] Kharazmi E, Zayernouri M, Karniadakis GE. Petrov-galerkin and spectral collocation methods for distributed order differential equations. *SIAM Journal on Scientific Computing*. 2017; 39(3): A1003–A1037.
[32] Doha EH, Abdelkawy MA, Amin AZM, Lopes AM . Shifted Jacobi-Gauss-collocation with convergence analysis for fractional integro-differential equations. *Communications in Nonlinear Science and Numerical Simulation*. 2019; 72: 342–359.
[33] Kilbas A, Srivastava HM, Trujillo JJ. *Theory and Applications of Fractional Differential Equations*. Amsterdam: Elsevier; 2006.
[34] Fahad HM, Fernandez A, Rehman MU, Siddiqi M. Tempered and hadamard-type fractional calculus with respect to functions. *Mediterranean Journal of Mathematics*. 2021; 18(4): 143.
[35] Fan EY, Li CP, Li ZQ. Numerical approaches to caputo-hadamard fractional derivatives with applications to long-term integration of fractional differential systems. *Communications in Nonlinear Science and Numerical Simulation*. 2022; 106: 106096.
[36] Li CP, Li ZQ. Stability and logarithmic decay of the solution to hadamard-type fractional differential equation. *Journal of Nonlinear Science*. 2021; 31: 1–60.
[37] Li CP, Li ZQ, Wang Z. Mathematical analysis and the local discontinuous galerkin method for caputo-hadamard fractional partial differential equation. *Journal of Scientific Computing*. 2020; 85: 1–27.
[38] Li CP, Li ZQ. On blow-up for a time-space fractional partial differential equation with exponential kernel in temporal derivative. *Journal of Mathematical Sciences*. 2022; 266(3): 381–394.
[39] Almeida R, Malinowska AB, Monteiro MTT. Fractional differential equations with a caputo derivative with respect to a kernel function and their applications. *Mathematical Methods in the Applied Sciences*. 2018; 41(1): 336–352.
[40] Izadi M, Veeresha P, Adel W. The fractional-order marriage-divorce mathematical model: numerical investigations and dynamical analysis. *The European Physical Journal Plus*. 2024; 139(3): 1–23.
[41] Nazari J, Heydari MH, Hosseininia M. Romanovski-jacobi polynomials for the numerical solution of multi-dimensional multi-order time fractional telegraph equations. *Results in Physics*. 2023; 53: 106937.
[42] Hafez RM, Abdelkawy MA, Ahmed HM. A refined spectral galerkin approach leveraging romanovski-jacobi polynomials for differential equations. *Mathematics*. 2025; 13(9): 1461.